Thermal Transitions in Polyimide Transfer Under Sliding Against Steel, Investigated by Raman Spectroscopy and Thermal Analysis

P. Samyn,[1] P. De Baets,[1] J. Van Craenenbroeck,[2] F. Verpoort,[2] G. Schoukens[3]

[1]*Ghent University, Laboratory Soete, Department Mechanical Construction and Production, Sint-Pietersnieuwstraat 41, B-9000 Gent, Belgium*
[2]*Ghent University, Laboratory of Organometallics and Catalysis, Department of Inorganic and Physical Chemistry, Krijgslaan 281 (S3), B-9000 Gent, Belgium*
[3]*Ghent University, Department of Textiles, Technologiepark 907, B-9052 Zwijnaarde, Belgium*

Received 22 July 2003; accepted 21 March 2005
DOI 10.1002/app.22395
Published online 4 May 2006 in Wiley InterScience (www.interscience.wiley.com).

ABSTRACT: Polyimides (PI) are known for their extremely high thermal stability and lack of a glass transition temperature below their decomposition point. Therefore, they are frequently used in high-demanding tribological applications. The tribological characteristics of sintered polyimide (SP-1) are presently investigated as a function of the sliding temperature that is artificially varied between 60°C and 260°C under fixed load in counterformal contact with a steel plate. For obtaining low friction and wear, a transfer film needs to develop onto the sliding counterface, induced by viscous polymer flow. As surface plastification is more difficult for high-performance materials, for example, polyimide, a transition towards low friction and stabilized wear rates is observed at temperatures higher than 180°C in accordance with the occurrence of plate-like transfer particles, while high friction and no transfer was observed at lower temperatures. This transition is correlated to a peak value in both friction and wear at 180°C and is further explained by Raman spectroscopy performed on the worn polymer surfaces and temperature-modulated differential scanning calorimetry. It is concluded that the intensity of C-*N*-C related absorption bands is minimal at 180°C and is complementary to the intensity of the C═C phenylene structure that is maximal at 180°C. The orientation of the C-O-C structure slightly decreases relative to the sliding surface at higher bulk temperatures. The amount of C═O functional groups is the lowest at 140°C, while its orientation progressively enhances at higher bulk temperatures. At 140°C also, the lowest wear rates were measured. The 180°C transition temperature with a peak value in both friction and wear corresponds to a secondary transition measured in the specific complex heat capacity, pointing out that the overall bulk temperature is presently more important than local flash temperatures for causing transitions in tribological behavior. © 2006 Wiley Periodicals, Inc. J Appl Polym Sci 101: 1407–1425, 2006

Key words: differential scanning calorimetry (DSC); polyimides; Raman spectroscopy; temperature; tribology

INTRODUCTION

The favorable use of polymer materials in dry sliding is indicated by their self-lubricating ability, with limited material transfer from the one rubbing surface to the other, induced by viscous flow. The mechanisms of transfer film formation[1] and its morphological properties resulting in low friction and low wear, characterize the reliability of a sliding couple that should be able to withdraw the applied dynamic stresses. A thin continuous film or "glaze" formed by orientation and shear of the polymer chains along the sliding direction yields the most favorable sliding characteristics. This type of transfer occurs most frequently for "smooth molecular profile" polymers, for example, polyethylene, with increased orientation at higher sliding velocities. For most polymers however, material transfer consists of a discontinuous film (nonuniform or lumpy transfer) with isolated particles adhering to the counterface and each particle progressively growing around a fixed nucleus. Then the performance of the tribological system is often reduced through vibrations and torsion within the sliding interface. The stability of each transfer particle depends on the force balance between both cohesive (mechanical resistance against particle detachment) and adhesive (attachment to the counterface by Coulomb interaction or Van der Waals bonding) forces. As long as the film particles remain permanently bonded, it cannot be considered as system wear, but it progressively converts metal/polymer contacts into polymer/polymer sliding.

Correspondence to: P. Samyn (Pieter.Samyn@UGent.be).
Contract grant sponsor: FWO (Flemish Research Fund).
Contract grant sponsor: Ghent University Research Board.

The concept that transfer allows the displacement of the shear plane within the soft transferred layer is true for homogeneous films. When shear or friction exceeds the cohesive forces within the film, the layer decomposes and adheres onto the polymer and the counterface surfaces as long as adhesive forces remain higher than the cohesive forces. Earlier theories by Hollander and Lancaster[2] prevail that transfer film depositions decrease the original counterface roughness and enhance the contact surface, resulting in lower stress concentrations and sliding interactions at the counterface asperities.

The tribological performance and transfer ability of polymer components strongly depend on the sliding temperature under frictional heating, controlling both materials' strength and transfer mechanisms. Higher temperatures increase the polymer chain moveability at the sliding surface due to weakening (lower cohesive forces) and allow for better orientation of the polymer chains. Moreover, temperature contributes to the transfer film thickness and adhesion, for example, through higher auto-adhesion of small dispersive particles on the metal surface, obtaining a more continuous film. Nowadays, tribological systems require high-performance plastics with high stiffness and increased thermal stability, for example, polyimides (PI), polyphenylene-sulfide (PPS), or polyetheretherketon (PEEK), where polymer transfer and orientation under shear forces occur less frequently because of the materials' high stiffness and thermal stability. Secondary transition temperatures are postponed or hardly appear, resulting in lower weakening tendencies where a component loses its load-carrying capacity.

Pioneering research on the tribological behavior of polyimides and their self-lubricating ability in film or bulk material has been performed by Fusaro[3] and Tewari and Bijwe,[4] mainly under vacuum conditions used for space applications. Nine different polyimides and their composites containing solid lubricants or fibers were studied, but the structures of only four types of PI were known; linear thermoplastics generally have higher wear rates than thermosettings. Their work indicates that the attainment of low friction depends on the transfer of a thin film of PI. According to some researchers, frictional transitions are correlated to transitions in wear, while others only observed a wear transition. Although frictional transitions are observed at higher temperatures, the reasons for it and relations with the polymer chain conformation remain difficult to illustrate. Orientation of aromatic structures occurs less frequently, while only specific functional groups or side-chains reorient without an overall alignment of the molecular backbone. Moreover, the presence of water molecules in moist air restricts the polymer chain relaxation by the formation of hydrogen bonds, becoming more pronounced under atmospheric sliding conditions. A close examination of the worn polyimide surface by Raman spectroscopy,[5] temperature modulated DSC measurement, and microscopic observation of the transfer film as presently performed, will provide additional information about the physical processes and orientation effects at the polymer surface during sliding.

EXPERIMENTAL

Tribotest configuration and sliding test conditions

Friction and wear tests were done on a cylinder-on-plate configuration in a PLINT TE 77 reciprocating test rig (Fig. 1) according to ASTM F732–98. A line contact between a polyimide cylinder (Ø 6 mm × 15 mm) and a fixed steel counterface (58 mm × 38 mm × 4 mm) was applied. The initial contact geometry was counterformal, although it continuously grew as wear proceeded, called an "increasing contact area" type of wear. The polymer sample (2) was fixed to the moving fixture (1) by a clamp (4) and a center mechanism (5), preventing it from rolling so that simple sliding was guaranteed. An oscillating motion of the polymer sample was provided by a controlled variable speed motor through an eccentric power transmission for the adjustment of the stroke, presently chosen at 15 mm. The stationary steel counterface (3) was connected to a base plate by means of four leaf springs (8) with high stiffness in the vertical direction and flexibility in the horizontal direction. A piezo-electrical force transducer (13) was used to measure the horizontal friction force. The vertical displacement of the cylinder towards its counterface was continuously measured by a contactless proximitor (14). However, because deformation by creep and thermal expansion interfere with wear depth measurements, weight measurements before and after the test were performed for obtaining "real" wear rates, that is, material loss. Sliding temperatures were measured by a DIN 43,710 K-type (nickel-chromium/nickel-aluminum) thermocouple (16) positioned on top of the steel counterface on a location distanced 10 mm from the outer end of the sliding stroke.

The sliding frequency was constant at 10 Hz, corresponding to a sliding velocity of 0.3 m/s. The normal load F_N was applied by a bridge (12) mechanically pulled down by rotation of a crank handle and transmitted onto the moving specimen by means of a roller bearing. The normal load was fixed at 50*N*. One test series was performed with free evolution of the contact temperature only resulting from frictional heating, either with or without air convection (15) in the climate box around the sliding zone to create a different temperature profile. For other tests, the steel counterface was heated at 60°C, 80°C, 100°C, 140°C, 180°C, 220°C, and 260°C by Vulstar heat cartridges (200 W, 400 Ω), continuously PID-controlled. All tests were

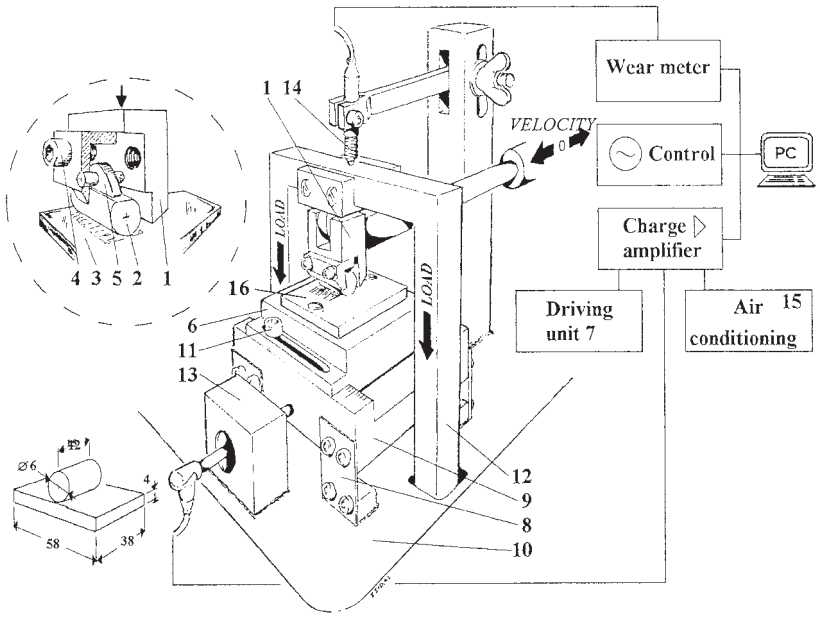

Figure 1 PLINT TE 77 cylinder-on-plate tribotester (numbers are explained in text).

performed under relative humidity RH = 60% within the climate box. The total sliding distance comprised 15 km. Test results of friction, wear, and bulk temperatures were calculated as an average of three separate test runs for each set of sliding parameters.

Contact conditions for the initial line contact are calculated in Table I according to the Hertzian theory,[6] with b the width of the wear track (15 mm) and R the cylinder radius (3 mm). When a normal load F_N is applied, an elastic deformation δ_H and an increase in static contact surface A_s result in a pressure distribution with peak and mean values as calculated from eq. (1):

$$p_{H,max} = \sqrt{\frac{(F_N/b)E}{2\pi R}} \quad p_{H,avg} = \frac{\pi}{4} p_{H,max} \tag{1}$$

The steady-state contact pressure obtained at the end of the sliding test for a cylindrical polymer specimen with radius R tested under normal load F_N is geometrically calculated from the wear depth Δh (measured by means of a micrometer), according to eq. (2):

$$p_{avg} = \frac{F_N}{A} = \frac{F_N}{b2\ell} = \frac{F_N}{b2\sqrt{R^2 - (R - \Delta h)^2}} \tag{2}$$

with A contact surface area and ℓ the semilength of the contact area in the sliding direction.

Test material

Sintered polyimide Vespel SP-1 is used as unfilled base resin from polycondensation between pyromellitic dianhydride (PMDA) and 4,4′ diamino diphenyl ether (ODA). The imide functionary group provides the polymer extremely high mechanical properties and thermal stability compared to other engineering polymers, for example, polyamides or polyacetals, with a long-term operational temperature of 310°C and short time resistance to 500°C. The resins have a

TABLE I
Contact Conditions Before and After the Sliding Tests

	Initial Hertz line contact				Steady-state contact (v = 0.3 m/s)					
					Free temperature	100°C	140°C	180°C	220°C	260°C
F_N (N)	$p_{H,avg}$ (MPa)	$p_{H,max}$ (MPa)	A_s (mm^2)	δ_H (μm)	p_{avg} (MPa)	p_{avg} (MPa)	p_{avg} (MPa)	p_{avg} (MPa)	p_{avg} (MPa)	P_{avg} (MPa)
50	30	38	1.7	2.5	1.38	0.96	1.13	0.93	0.87	0.89

crystalline content between 25 to 50%, resulting in a density of 1.34 g/cm^3 and an E-modulus of 2480 MPa at 23°C decreasing to 1450 MPa at 260°C. Sintering the polyimide after chemical reaction provides them semi-thermoset characteristics. As such, there is not revealed any transition temperature, and mechanical properties decrease only slightly linearly with higher temperatures with a 24 MPa compressive stress. They do not melt as thermoplastics, but show progressive oxidative degradation. Extreme pv-limits up to 1.7 MPa m/s for SP-1 (corresponding to wear rates k = 34.10^{-7} mm^3/Nm) are reported,[7] not exceeding a surface temperature of 340°C.

The counterface plates are made of hardened and tempered 40 CrMnNiMo8 steel (DIN 1.2738) with chemical composition as follows in (wt %): C = 0.43%, Si < 0.30%, Mn = 1.50%, Cr = 2.00%, Mo = 0.20%, Ni = 1.10%, with hardness of 300 HB and surface roughness R_a = 0.10 μm, measured perpendicular to the sliding direction and obtained by polishing with an SiC-paper (grid 600). The roughness is chosen relatively low because polyimides do not perform well under abrasive conditions and ground surface finishes are preferred above turned surfaces.

Fourier transform Raman spectroscopy

The polyimide surfaces before and after sliding under 50*N* at different temperatures are characterized by Raman spectroscopy. Measurements are performed on a Bruker FT spectrometer Equinox 55S (Bruker Optik, Ettlingen, Germany), equipped with a Raman module FRA 106 fitted to a nitrogen cooled (77 K) germanium high sensitivity detector D418-T. The applied laser wavelength during the experiments was the 1.064 μm line from a Diode Laser Pumped Nd: YAG laser. All spectra are recorded at a resolution of 3 cm^{-1} using a nonfocused laser beam with a power of 70 mW. Each spectrum is collected as an average of 250 scans, so that the applied parameters result in an optimum noise/intensity ratio for all spectra. The dispersion of the spectrum over the total sliding surface is little. A quantitative interpretation of the spectra in the 500 cm^{-1} to 2000 cm^{-1} frequency range is made using the baseline theory for correction of the individual spectra. Normalized percent relative intensities should be used to compensate for any change in experimental conditions, such as excitation intensity, and sample positioning.

Differential scanning calorimetry (DSC) measurements

The thermal transitions in polyimide SP-1 are investigated by a 2920 Modulated DSC (TA Instruments). Those measurements include a thermomechanical analysis by recording the difference in heat flow between the polymer test sample and a reference material under heating. In a traditional DSC, the temperature profile is programmed as a linear function of the time. This method is frequently used for determination of glass transitions, melting temperatures, or heat capacities, although it is less sensitive to secondary transitions as occur in polyimides. Therefore, the sample is subjected to a modulated temperature profile (M-DSC), with a periodic (sinusoidal) heating rate superimposed to the linear heating rate. The measured heat flow in response to this temperature program is also periodic due to the immediate high heating rates implied by the periodic signal. Certain effects, such as changes in the specific heat capacity, can follow the applied heating rate ("reversing" phenomena), whereas other effects, such as crystallization, cannot ("irreversible" phenomena). The periodic heat flow signal *H* is, therefore, the superposition of an in-phase heat flow component and a component that is out of phase with the heating rate. Schawe[8] has proposed that the data obtained using a periodic temperature profile may be best interpreted in terms of a complex heat capacity $C_p^* = C' - iC''$, where the C′ component originates from the component of heat-flow that is in-phase with the temperature modulation and the C″ component out of phase arises from enthalpy dissipation processes. The response to the linear temperature part (DSC) yields the *total heat capacity*, while the response to the modulated temperature part (M-DSC) yields the *complex specific heat capacity* c_p^*,[9] according to eq. (3):

$$|c_p^*| = \frac{1}{m}\left(\frac{dH}{dT}\right) \tag{3}$$

Measurements are performed under a nitrogen atmosphere at a scanning rate of 10°C/min in the temperature range of 20 to 400°C. Test samples are approximately 6 mg. The calibration of the temperature and the heat flow scales at the same heating rate is performed with In, Zn, and Sn.

RESULTS

Friction and bulk temperature measurements

The coefficients of dynamic friction are measured for a normal load of 50*N* and a sliding velocity of 0.3 m/s under variable sliding temperatures. In tests with a free evolution of the contact temperature, the temperature rise only results from dissipation of frictional energy. A second temperature profile is applied through cooling the counterface by convection around the contact zone. For both conditions, the evolution of measured friction and measured bulk temperature with sliding distance is shown in Figure 2a, with rather stable friction (μ_{dyn} = 0.49) in the case of cool-

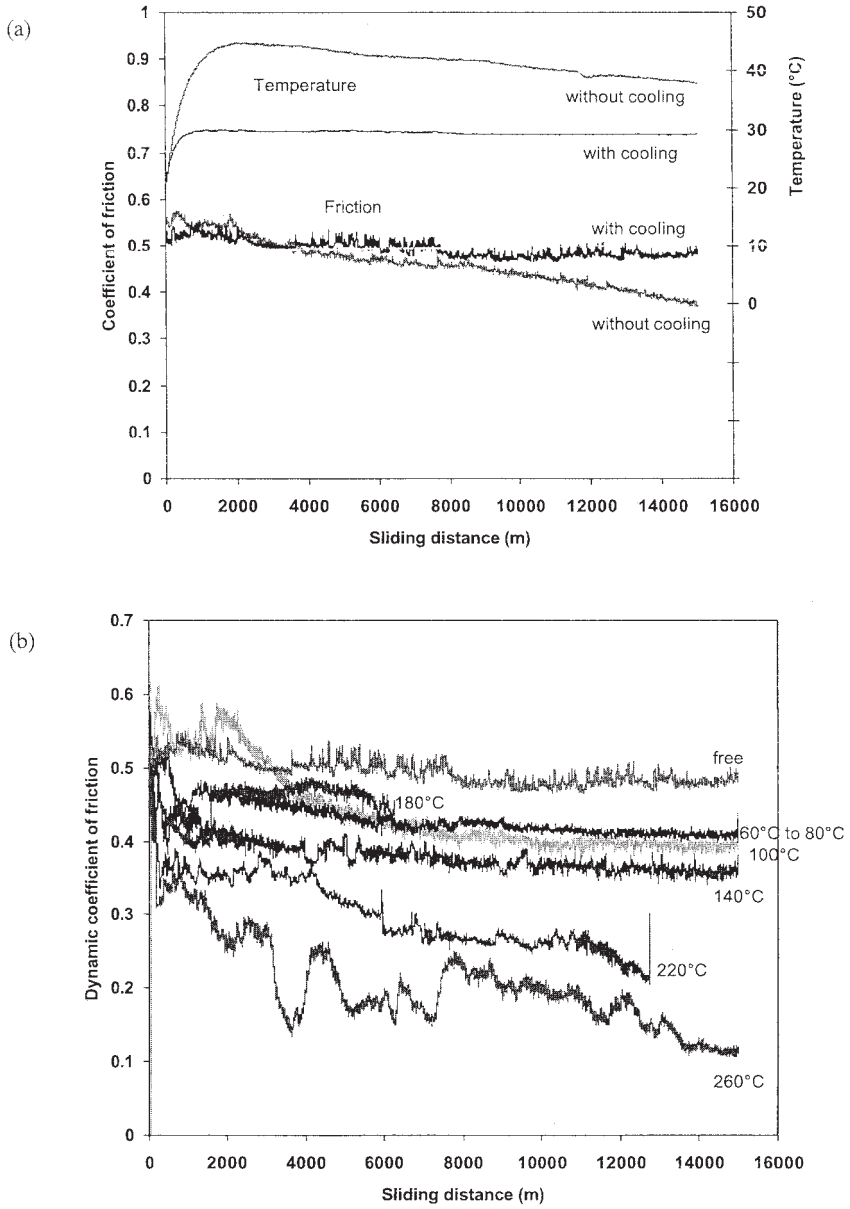

Figure 2 Coefficient of friction as a function of the sliding distance, for (a) free temperature with and wthout cooling, (b) controlled temperature.

ing the test environment and a steadily decreasing friction (μ_{dyn} = 0.37) in the case of free temperature. The slightly higher temperature (> 40°C) enhances lower friction, although it becomes less stable and progressively decreases. According to Loewen and Shaw,[10] the maximum and mean rise in bulk temperature at the sliding interface can be estimated as a function of the frictional power q = μ p v (μ = coefficient of friction, p = contact pressure, v = 0.3 m/s) and the aspect ratio of the surface area (b/ℓ), from an analytical approach according to eq. (4):

$$\theta_{max} = A_{max}\frac{q\ell}{k} \quad \bar{\theta} = \bar{A}\frac{q\ell}{k} \tag{4}$$

with A_{max} and $\bar{A}$ the area factors (given as a function of the aspect ratio of the surface area[10]), k taken as the steel thermal conductivity (= 33 W/(mK)), and ℓ the semilength of the contact area in the sliding direction. As the nominal contact area and contact pressure are continuously changing due to wear, the question rises as to which conditions should be used for the calculations. While the contact conditions calculated from the Hertzian elastic theory are only true for a short time of sliding, that is, as long as no wear occurs, the conditions for estimating bulk temperatures are taken from the experimentally measured steady-state data in Table I. In the case of free temperature rise, the mean bulk temperature $\bar{\theta}$ equals 35°C and the maximum

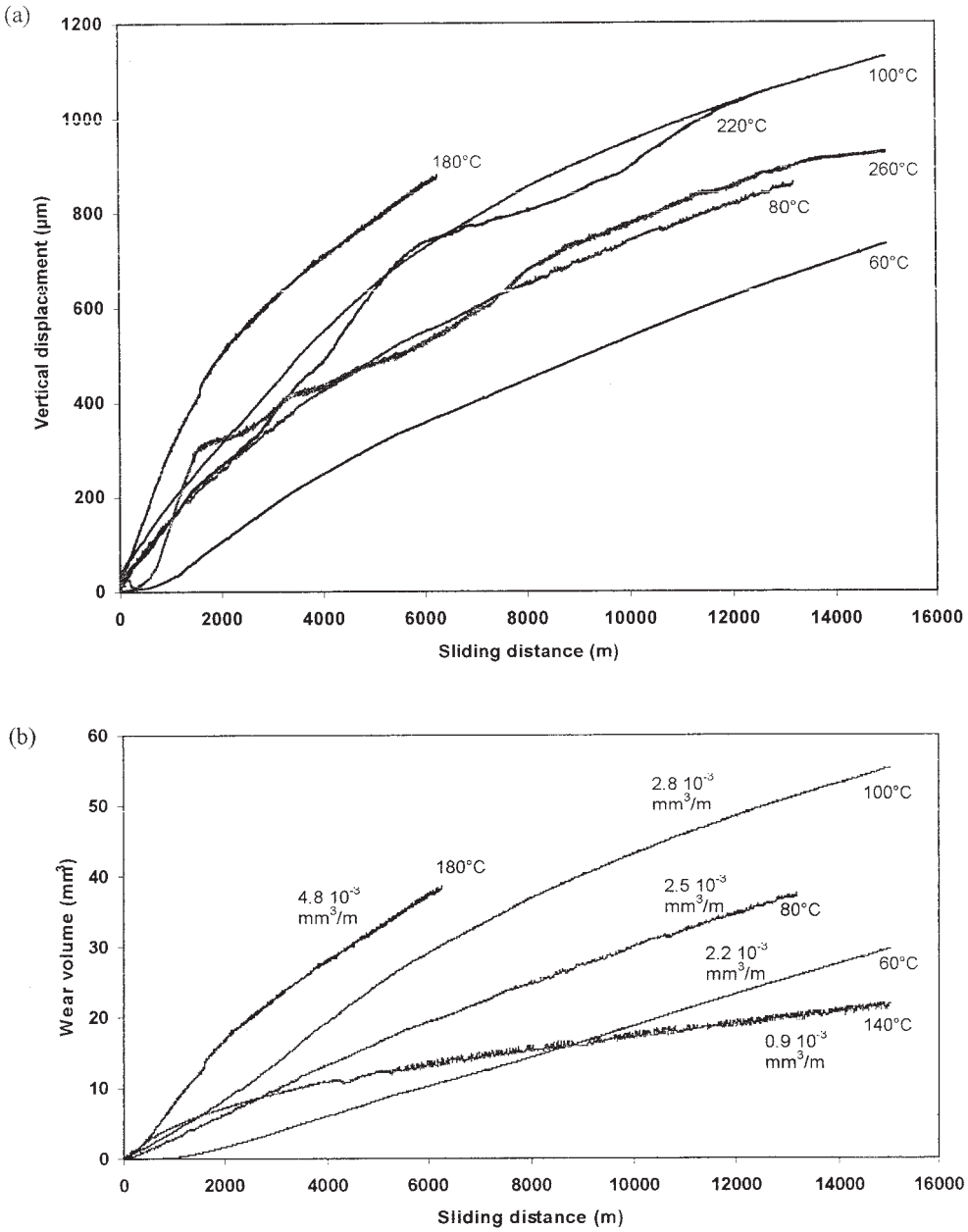

Figure 3 Wear graph as a function of the sliding distance for tests under controlled temperature, characterizing material loss and deformation: (a) recorded vertical displacement, (b) volumetric wear rate calculated from vertical displacement and calculated wear rates.

bulk temperature θ_{max} equals 39°C under steady-state. These values are in good correspondence with the measured temperature of 38°C at the end of the sliding test, as plotted in Figure 3(a). Under cooled atmosphere, calculated temperatures should rise towards $\bar{\theta}$ = 39°C and θ_{max} = 41°C because of higher friction. However, cooling air results in a lower measured bulk temperature through convection. In any case, the bulk temperatures calculated and/or measured above remain below those that are artificially implied to the steel counterface by heating in the following tests.

Figure 2b shows the friction measurements in case the counterface is heated at temperatures between 60°C and 260°C. As the presently applied temperatures govern over the total contact area, they are also indicated as "bulk temperatures." The friction curves are characterized by the occurrence of both a running-in and a steady-state phase, with running-in effects becoming more pronounced at elevated sliding temperatures. Running-in is a process whereby the friction coefficient starts out high and then drops to some lower value due to orientation taking place at the sliding interface. The initial peak in friction was also observed by Tanaka and Ueda[11] under unidirectional sliding and was explained by the increase in real contact area and decrease in surface roughness through

TABLE II
Determination of Wear by Weight and Dimensional Measurements

Applied bulk temperature (°C)	Dimensional measurements		Weight measurements		Difference %
	Δh (mm)	mm^3	Δg (g)	mm^3	
60	0.45	14.45	0.0208	15.52	−7.0
80	0.57	20.47	0.0247	18.43	11.1
100	0.55	19.42	0.0236	17.61	10.3
140	0.39	11.69	0.0146	10.90	7.2
180	0.60	22.08	0.0283	21.11	4.5
220	0.70	27.66	0.0354	26.42	4.5
260	0.65	24.82	0.0310	23.13	7.3

the formation of a transfer film. The latter causes a competition between a higher adhesive component of friction and reduced plowing interaction. However, the initial friction peak is presently attributed to geometric effects with a change in contact pressure (increase in contact area) and deformation of the initial line contact during the test course. In contrast, friction and wear tests performed by Chitsaz-Zadeh and Eiss[12] on a pin-on-disc configuration (conformal contact) showed an initial period of very low friction, which was abruptly terminated by a rise in friction and simultaneous appearance of wear debris at steady-state. This behavior is an indication of fatigue wear, with the incubation period observed to be characteristic for the polyimide structure. In present sliding tests, the coefficients of friction decrease progressively with increasing sliding distance towards a steady-state value that is obtained after ± 4000 m of sliding because of the leveling of contact pressures. However, stabilization occurs with more difficulty at higher temperatures.

As examined in the next sections, low friction occurs due to possibilities of transfer film formation above 180°C. The first heating step of 60°C provides nearly identical frictional conditions as a previous test under free temperature. A further increase in sliding temperatures results in lower friction, except at 180°C where a sudden increase in friction occurs after 1600 m of sliding. This transition will be further explained throughout the following discussion related to transfer film formation and molecular orientation effects.

Wear measurements

The vertical displacement of the polymer cylinder towards its counterface is continuously recorded as shown in Figure 3(a), representative for both wear (real material loss) and deformation or creep. The sharpest increase in vertical displacement is recorded for the 180°C bulk temperature. Higher temperatures result in lower and less uniform vertical displacement. These perturbations result from interactions with wear debris accumulation at the sliding interface. Most of the small-scale tests under elevated temperature show linearly increasing wear depth with sliding distance; but at temperatures of 220°C and 260°C, there are revealed running-in effects with higher wear rates and a transition towards lower steady-state wear after certain sliding times. They may result from interference with transfer film formation, even causing strong variations in the wear rate during the test course. Volumetric wear rates ΔV are calculated in Figure 3(b) from wear depths Δh (ΔV proportional to $\Delta h^{3/2}$), revealing more evidently running-in and linearly increasing steady-state periods, with the wear rate calculated from the respective trendlines. A transition occurs between 100°C and 200°C, with a minimum wear rate at 140°C and a maximum wear rate at 180°C.

Real wear or material loss is determined from the weight loss of the polyimide samples before and after testing, and is compared to dimensional measurements of the polymer cylinder height in Table II. The equivalent wear volume of cylindrical polyimide samples (radius R, width b) from wear depths Δh are calculated according to eq. (5):

$$b\left(R^2 \sin^{-1}\frac{\sqrt{R^2-(R-\Delta h)^2}}{R} - (R-\Delta h)\sqrt{R^2-(R-\Delta h)^2}\right) \quad (5)$$

The data reported here pertain to the wear volumes over the whole test period, including both an eventual running-in period and steady state conditions. It is clear that the height reduction of the polymer sample results in a higher equivalent wear volume compared to the equivalent wear volume calculated from weight reduction, because of viscoelastic deformation of the test cylinder under load. However, these discrepancies gradually decrease from 11% at 80°C to 4.5% at 220°C, possibly due to water desorption at higher temperatures, as explained below. When the dimensionally measured wear depths Δh are compared to the vertical displacement in Figure 3, their ratio is between 0.60 to 0.70 because the additional deformation (creep) during sliding is recovered after the load has been removed.

DISCUSSION

Bulk temperature and flash temperature

Frictional interactions are energy dissipating processes where the mechanical energy input for establishing the relative movement is partially converted into heat. Through hysteresis effects caused by the viscoelastic polymer properties (elastic-plastic deformation), there is approximately 90% of the total energy input transformed into heat, leading to an increase in contact temperature. The tribosystem contact temperature is, therefore, determined through the combination of the ambient temperature, the temperature externally applied to the contact surface, and frictional heating caused by a moving heating source. The resulting temperature distribution at the contact area mainly depends on the sliding velocity, contact pressure, coefficient of friction, thermal conductivity of the mating materials, contact geometry, and surface roughness, and contains an overall bulk temperature and a local flash temperature.

The temperatures presently applied at the contact surface and measured by means of the thermocouple equal *bulk temperatures* as they represent an average value uniformly across the entire sliding counterface under steady-state conditions. Its value results from the total energy input (temperature + friction) and the dissipation of energy on a macroscopic scale (conduction, convection, and radiation). A steady-state temperature establishes after certain sliding times, depending on the thermal conductivity and bulk geometry of both sliding materials. As present steel conductivity (33 W/mK) is much higher than the polyimide conductivity (0.29 W/mK), most of the frictional energy is dissipated by conduction through the steel counterface or by convection. The bulk temperature (average surface temperature) is a good estimation for the contact temperature up to 10 μm under the sliding contact and was calculated in the previous section by the Loewen and Shaw model.

The microscopic contact between two sliding partners is concentrated at few individual roughness asperities, with the real area of contact much smaller than the apparent area of contact. The real heat flow should, therefore, be regulated through discrete contact spots, resulting in locally high contact temperatures, called the *flash temperature*, as introduced for the first time by Blok.[13] The energy is locally dissipated in an extremely short period (0.001 s), during which the melting or degradation temperature of the polymer can be exceeded, without a real heat flux towards the neighboring contact areas. It is reported that these temperatures can have a critical influence on the frictional and wear characteristics because of change in mechanical, chemical, and thermal properties of the sliding surfaces; although elementary calculations show that this temperature flash component is limited to the material immediately at 5 to 10 μm below the contact surface and that it decays in a fraction of the sliding motion. It is experimentally measured for present sliding tests with controlled bulk temperature between 80°C and 260°C that the input of frictional energy (which is proportional to the coefficient of friction μ, the contact pressure p, and sliding velocity v) in addition to the bulk temperature does not result in any increase of the externally applied bulk temperature, as measured by the thermocouple. The frictional energy should therefore be locally dissipated in the contact zone, resulting in an increase of the flash contact temperature.

Several models are available for calculation of flash temperatures (e.g., Archard,[14] Tian-Kennedy,[15] Greenwood,[16] and Ashby[17]), while large discrepancies in the results can be obtained for the same contact situation mainly depending on the assumptions about the real contact area, changes in thermal properties of the tribological interface, coefficient of friction, and roughness profile. Based on the available information obtained from present sliding tests, a temperature model developed by Jaeger[18] is presently evaluated for estimating the flash temperature θ_f from eq. (6):

$$\theta_f = 0.236 \frac{\mu F_N \nu}{\ell (k_1 + k_2)} \tag{6}$$

with μ the coefficient of friction, F_N normal load, v sliding velocity, ℓ semilength of contact surface in the sliding direction, and k_1 or k_2 the thermal conductivity of the steel (= 33 W/(mK)) and polyimide (= 0.29 W/(mK)), respectively. As friction results in a temperature rise of the contact temperature relative to the original counterface temperature, the rise in flash temperature is superimposed on the environmental temperature of 25°C in the case of free contact temperature or is added to the applied bulk temperature in the case of temperature controlled sliding tests for calculating the maximum contact temperature. The Jaeger model is developed for a moving heat source as a single-contact asperity and assumes that the heat conduction into a semi-infinite solid is one-dimensional. The solution is obtained for strip or square heat sources and is based on graphical results. Calculations under a free temperature result in a flash temperature of 53°C and for a cooled atmosphere 63°C. It is clear that those temperatures are higher than the measured and calculated values above, although remaining below the temperature of 80°C that is artificially applied in a first heating step. An overview of the flash temperatures and locally dissipated frictional energy (J/s) for the temperature controlled sliding tests is given in Table III, with the maximum calculated contact temperature remaining below the reported long-time exposure temperature limit of 310°C.[19]

TABLE III
Calculation of the Flash Temperatures for Tests Under Controlled Temperature

Applied bulk temperature (°C)	Semi-contact length (mm)	Locally dissipated frictional energy $\mu F_N v$ (J/s)	Local rise in flash temperature (°C)	Maximum contact temperature (°C)
60	1.58	6.3	119	179
80	1.76	6.1	104	184
100	1.73	6.0	104	204
140	1.48	5.4	110	250
180	1.80	6.8	112	292
220	1.93	4.1	63	283
260	1.86	3.0	48	308

Relation between friction, wear rate, and temperature

Figure 4(a,b) show the average coefficient of friction and the wear rate as a function of the bulk temperature. There are revealed two friction regimes depending on the temperature, with a clear transition above 180°C. At the end of the sliding test, high friction (μ_{dyn} = 0.35 to 0.40) is found at lower temperatures and low friction (μ_{dyn} = 0.20 to 0.27) is found at higher temperatures. Friction decreases progressively at higher temperatures, but a peak value at the transition temperature of 180°C starts to develop after 100 m of

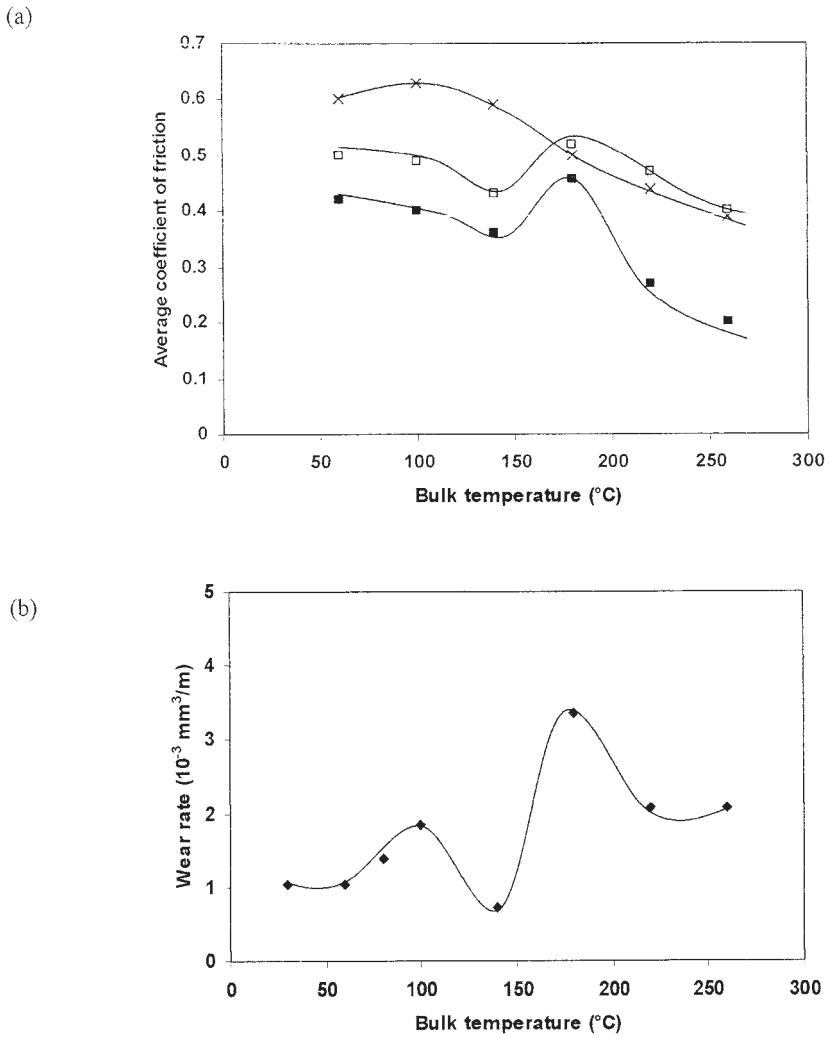

Figure 4 Temperature dependence of (a) average coefficient of friction at different sliding distances: (x) 30 m, □ 100 m, ■ 15,000 m; (b) wear rates calculated from weight loss (♦ 15,000 m).

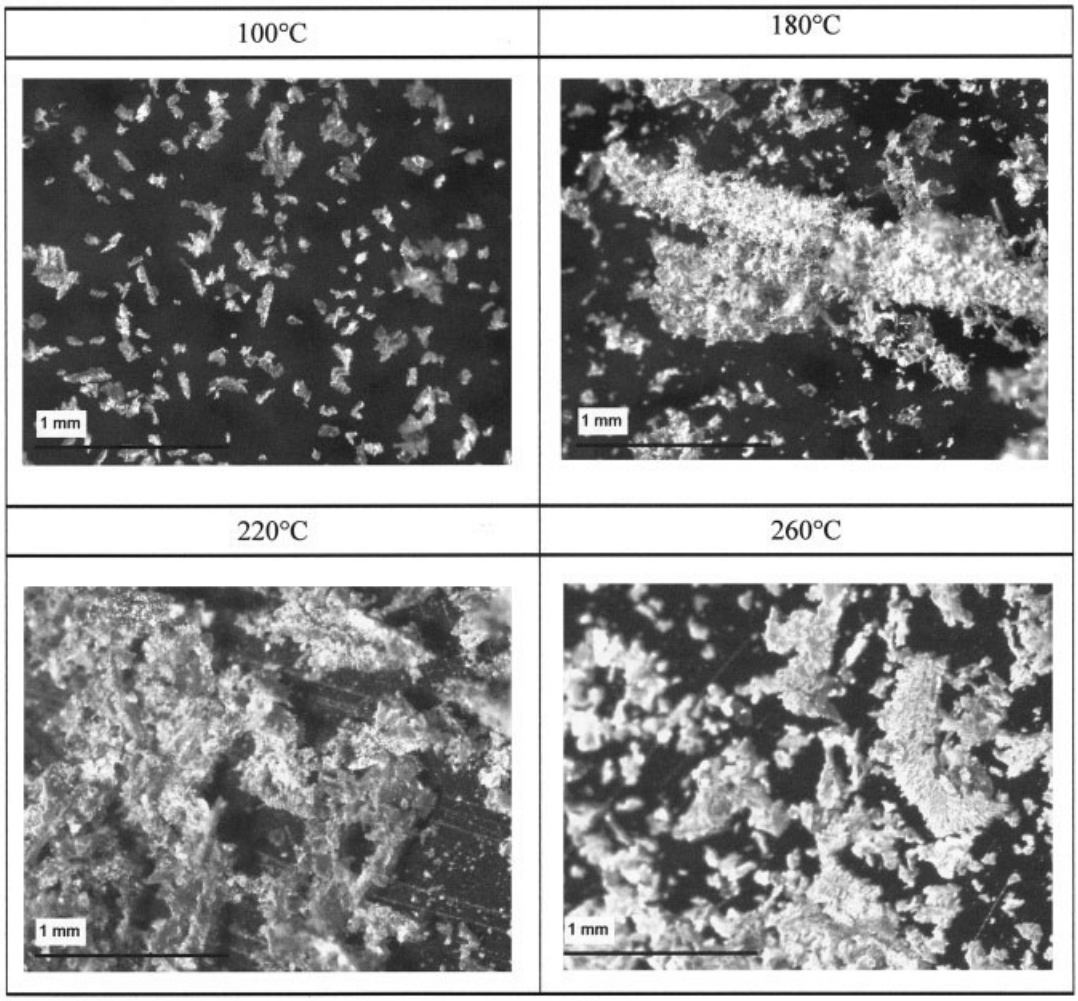

Figure 5 Optical microscopy of collected wear debris after sliding at different bulk temperatures.

sliding. The present transition is more evident than findings of Iwabuchi et al.[20] investigating SP-1 under fretting conditions. At ambient pressure of 10^5 Pa, they observed slightly higher coefficients of friction above 200°C, although this trend diminished at the end of the sliding test towards constant friction as a function of temperature. The significant difference between fretting and reciprocating sliding is that wear debris is not removed from the interface, permitting the transfer of polyimide to an opposing surface with ease even at low temperature. Under unidirectional sliding, however, Tanaka and Ueda[11] also found higher steady-state coefficients of friction above 200°C owing to the type of transfer. The present transition in friction corresponds to a transition in wear, with a maximum wear rate of 3.37 10^{-3} mm^3/m at 180°C. It is clear that high temperatures do not imply a transition from a mild towards a severe wear regime, but rather cause a stabilization in wear rates. The low wear rate at 140°C corresponds to low vertical displacements Δh in Figure 3. In contrast, Cong et al.[21] found higher wear rates with increasing temperature for thermoplastic polyimides.

Tewari and Bijwe[4] also observed a peak in both steady-state friction and wear, with the position of the transition peaks depending on the sliding speed: while the friction peak occurred at 150°C, it seems not correlated to the wear peak that occurred at 200°C. They reported that the color of wear debris varied with increasing temperature and became very dark at the temperature near the wear peak, indicating that thermal decomposition should be responsible for transitions and wear peaks. As decomposition is expected to occur only at 500–700°C,[22,23] other theories about the friction and wear peak should prevail. Optical microscopy of present wear debris (Fig. 5) shows no evidence of thermal degradation after sliding under the highest temperature in air, although it is clear that the wear debris morphology depends on the sliding temperature, with only small particles observed after sliding under 100°C bulk temperature. The detached particles become larger at temperatures above 180°C

and even reflect the original sintered structure, consisting of a grain-sized structure of separate polyimide powder particles that are agglomerated within larger debris particles.

This morphology change can explain the maximum in wear rates at 180°C, since it was noted by Fusaro that the transferred particles might act as an abrasive, with the fine particles more harmful than the large ones, acting as a contaminant. Where large particles occur, wear rates decrease or stabilize. Slight plastification is only observed at 220°C and 260°C as some of the particles are glossy and become squeezed into the contact zone under shearing forces. As no thermal degradation of the wear debris at temperatures above 200°C is presently observed, the transitions in friction and wear properties might be caused by structural changes.

Matsubara et al.[24] explained the peak value as an interaction between the increase in abrasive action and the chemical changes of the polyimide with increasing temperature. Tanaka and Yamada[25] discussed that the peak was related to the amount of transferred film, which could reduce wear. The effect of moisture in air on the tribological properties of a polyimide film was examined by Fusaro.[26] He showed that the transition temperature, at which the coefficient of friction decreases, increases in moist air, and the coefficient of friction at temperatures below the transition temperature is lower in moist air. Wear rates at high temperatures are greater in moist air. The transition was found to occur in inert atmosphere (dry argon, $<$20 ppm H_2O) or in dry air ($<$20 ppm H_2O) at 40 $\pm$ 10°C. When water vapor was present in the air (10,000 ppm H_2O), the transition was prevented or shifted upwards to "somewhere" between 100°C and 200°C.

In the case of semicrystalline PI, as present Vespel SP-1, the transition should manifest more pronounced than in the case of amorphous PI. As polyimide can absorb moisture, the absorbed moisture presumably reduces the bond strength and restricts the polymer chain moveability. The transitions in friction mechanisms found by Fusaro were attributed to the higher polymer chain mobility and orientation effects at the surface in the absence of water, leading to a texture conducive to easy shear. Such a texture could be produced by an extended chain molecular structure with the chains parallel to the sliding direction. In parallel, bulk temperatures between 100°C and 200°C as presently applied are able to break the hydrogen bonds and reduce the absorbed moisture by liberating water at the sliding interface. From that moment on, molecular reorganization becomes possible, resulting in lower friction. At temperatures below the transition, this reordering cannot occur since the molecules do not possess the degree of freedom necessary for rotation. However, the transition in friction was not necessarily correlated with transitions in wear. Bill[27] reported that wear of polyimide in moist air was greater than that in dry air without change in friction.

Optical and SEM microscopy of steel counterface after sliding

The formation of a polymer transfer film on the steel counterface as studied by optical microscopy revealed that there is no evidence of polymer transfer onto the steel counterface in cases of free counterface temperature. Also, at controlled temperatures below 180°C, no polymer transfer films are detected. As shown in Figure 6, only small separate wear debris particles collect into the grooves of the steel counterface during sliding at 100°C, visible as black points into the roughness grooves on the steel counterface. Higher temperatures of 180°C, 220°C, and 260°C cause the formation of a polymer transfer film in increasing amount with higher temperatures. However, SEM-microscopy in Figure 7 revealed that the transfer films remain discontinuous, and in none of the cases is there found a thin and homogeneous transfer film.

The transfer at temperatures of 180°C, 220°C, and 260°C seems to be characterized by particles smoothed over the entire sliding surface and large patches of powdery material drawn into plate-like sheets. The latter morphology becomes more important at higher temperatures, as weakening allows for plastification of the transferred particles, which does not happen to the separate transferred wear debris particles at 100°C. Although the transfer film is beneficial for lower friction, its formation causes huge instabilities, as seen in sliding under 260°C on Figure 3(b). They result from subsequent melting of transferred polymer parts, removal out of the contact zone, and the local formation of a new film. Energy dispersion spectroscopic (EDS) analysis on the transferred polyimide parts compared to the original steel counterface indicates that the transfer areas are enriched of carbon, nitrogen, and oxygen (Fig. 8). All of the elements of the polyimide samples are transferred onto the steel counterface. Other elements, as iron, chromium, manganese, and nickel, represent the high-alloy steel type.

The change in transfer behavior and morphology of the wear surface reflects a change in friction and wear mechanisms. Also, Fusaro[26] observed two different regions depending on the test conditions. The appearance of island and overall transfer regimes resembles spallation and brittle fracture, respectively. In the case of island transfer, there were abrasive grooves on the surface and many fine particles at the slip end. The

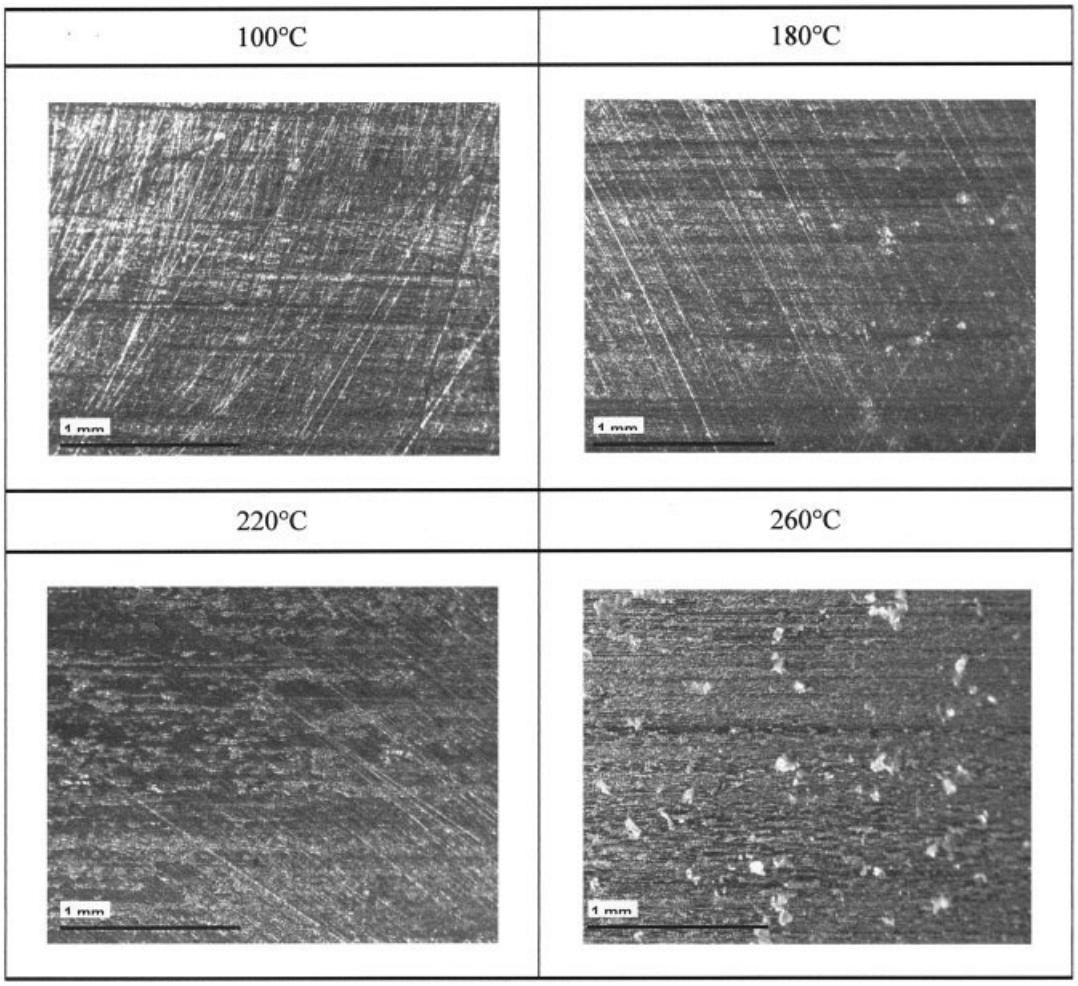

Figure 6 Optical microscopy of the transfer film formation on the steel counterface after sliding at different bulk temperatures.

transferred particles then act as abrasive. Where overall transfer occurred, the abrasive pattern was not detected. On the other hand, Matsubara[24] performed SEM studies of the counterface that indicated very little transfer of polymer at the transition temperature. It was therefore suggested that while synthesizing polymer, some unreacted monomers were left behind. As the sliding temperature increased, the residual monomers could undergo intramolecular condensation, resulting in additional imidization and thus generating H_2O vapor as a condensation product while sliding at high temperatures. Furthermore, decomposition of the –COOH group of the unreacted part of the polymer chains might take place with breaking of the PI chain and generation of CO_2. Both H_2O and CO_2 suppress the formation of a transferred film. Further increase in temperature decreased the wear rates and the friction, which could be due to a thicker transferred polymer layer at high temperature. Tanaka and Yamada[25] considered, therefore, that the peak in wear was related to large transfer at high temperatures reducing wear.

Raman spectroscopy of the polyimide sliding surfaces

Properly explaining the physicochemical reactions at the sliding counterface, Raman spectroscopy has been applied to the worn polyimide surfaces shown in Figure 9. Vibrational spectroscopy is an effective probe to assess the nature of chemical bonding, interactions, conformations, and even orientation of molecules. However, this technique has been rarely applied on semithermoset bulk polyimide for correlating the observed transitions in friction and/or wear between 100°C and 200°C. Most Raman characterization of polyimide was performed on thermoplastic films after low-force cloth rubbing.[28] Absorption bands can partially be assigned to PI (polyimide) and its unreacted precursor PAA (polyamic acid), as summarized in Table IV. Their identification results from studies on the imidization process of PAA into PI, where the amide-related bands disappear and the corresponding imide-related bands appear as the heating temperature increases. In more detail, the respective bands for

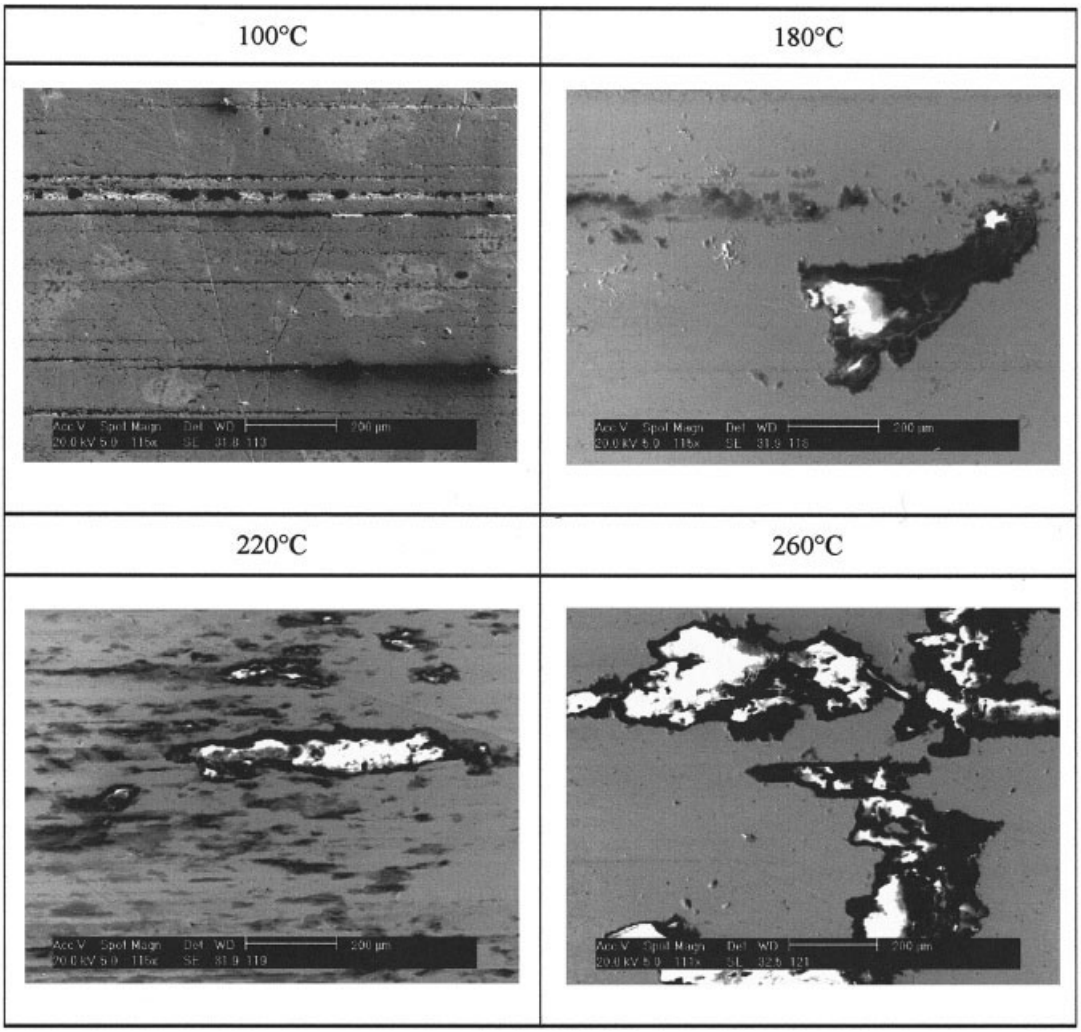

Figure 7 SEM microscopy of the transfer film after sliding at different bulk temperatures.

carboxylic acid and amide II at 1330 cm^{-1} and 1565 cm^{-1} gradually diminish and finally disappear at 250°C. Conversely, the typical imide peaks at 1395 cm^{-1} and 1786 cm^{-1} begin to appear at 80°C and grow up to 250°C. The imide I vibration is characteristic for the C═O stretch, while imide II and imide III vibrations correspond to the axial and transverse stretch of the C-*N*-C bonds. Other typical bands for amic acid and imide behave in the same manner as those of PAA and PI, respectively. Therefore, it is valuable to investigate the relative intensity changes for monitoring decomposition (relationship between amide/imide bands) or orientation (relationship between imide bands) during sliding. Walsh et al.[29] made a more theoretical study on the flexibility of different bonds in the polyimide PMDA-ODA structure.

A reference spectrum of the unworn polyimide SP-1 is shown in Figure 10. Typical D (1340 cm^{-1}) and G (1580 cm^{-1}) bands, characteristic for crystalline graphitic carbon, are not observed as was done by, for example, Raimondi et al.[30] after ion radiation. It means that no degradation of the polyimide after sliding tests presently occurs. The variation in relative intensity of some characteristic Raman bands is shown in Figure 11 as a function of the applied bulk temperature. Although it was previously mentioned by Ge et al.[31] that normal FT-Raman spectra for thick polyimide films are not strongly affected by rubbing because of sensitivity lack, the following trends become clear:

Formation and/or decomposition of imide from PAA

From the spectra in Figure 10, it is clear that some of the amide-related bands do not occur due to the relatively large conversion of PAA into imide. According to Han Yu et al.,[32] studying effects of thermal treatments on thin films between 80°C and 350°C, the imide cyclization is characterized by positive cross peaks at 1565, 1601 cm^{-1} and negative cross peaks at 1601, 1786 cm^{-1}. It means that their intensity in a one-dimensional spectrum varies in the same or opposite direction as a function of the heating temperature. As it is known that the imidization

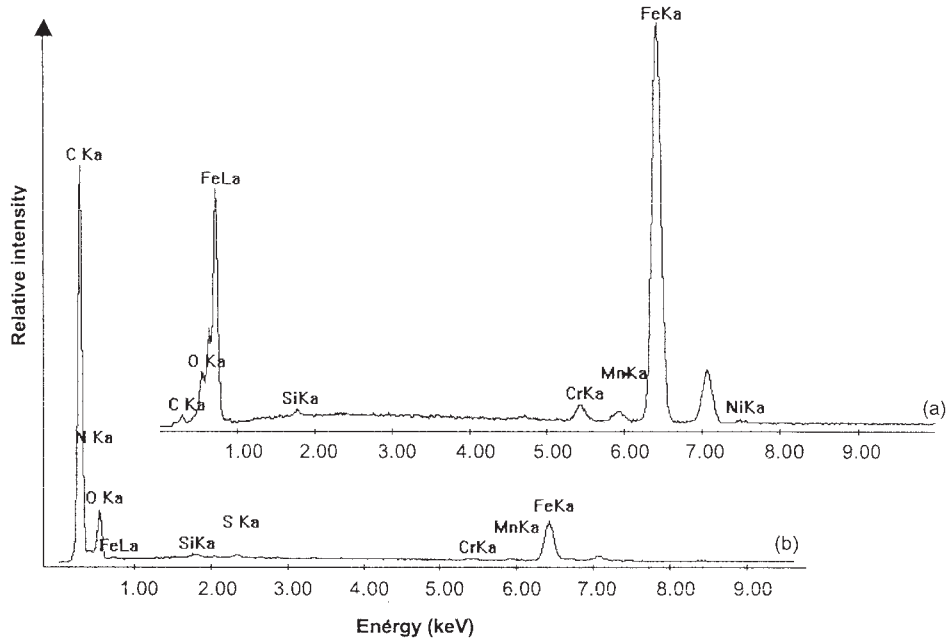

Figure 8 EDS spectrum of the steel surface: (a) original, (b) polyimide transfer depositions after sliding at 260°C.

of SP-1 is not complete after chemical reaction, present sliding tests may induce further thermal imidization from PAA into PI. This is ascertained by the change in relative intensity of the 1612/1601, 1786/1601, and 1395/1601 bands, indicating an increasing amount of imide with increasing sliding bulk temperature. However, their relative intensities are discontinuous at sliding bulk temperatures between 100°C and 180°C, with a minimum value of the aromatic dianhydride vibration (1612 cm^{-1}) and *C-N*-C axial vibration (1395 cm^{-1}) in the polyimide part at 180°C, pointing towards minimized ring closing reactions at this temperature. At higher temperatures, the reaction towards polyimide develops again.

Previously it was found by Ge et al.[31] that rubbing monotonously enhances the vibration mode at 1612 cm^{-1}, representing the aromatic in-plane ring stretching in the dianhydride. This suggests that rubbing should cause the phenylenes in the dianhydride part of the polyimide backbones to more or less tilt away from the surface, although present discontinuity at 180°C is in accordance with the peak value in friction and wear [Fig. 4(a)]. The sharp decrease of the 1786/1601 intensity at 140°C, possibly related to decomposition or disorientation of the C═O group in the polyimide, can explain the low wear rates measured at this temperature [Fig. 4(b)].

Orientation effects of functional groups in imide structure

The orientation within the imide structure is given by the relative intensities of the imide-related functional groups. With the 1612 cm^{-1} band chosen as a reference band correlated to the aromatic ring structure, it permits demonstrating the orientation of different functional groups relative to the imide phenyl ring. At higher temperatures, the 1786 cm^{-1} peak grows progressively. This indicates that the C═O group in the imide ring becomes progressively more stretched through the combination of increased temperature and applied shearing stress, which yields the possibility for molecular orientation at the sliding surface. Fukura[33] investigated the thermally activated structural changes in polyetherimide by internal friction and also concluded that relaxation induced an important C═O motion. Phenomena concerning molecular relaxation enhance the moveability of certain segments in the molecular structure, although the orientation of C═O side groups remains constant between 100°C and 180°C due to the restrictions implied by the chemical reactions described above. At higher temperatures, these restrictions vanish and further orientation happens.

Present orientation and increase in the 1786 cm^{-1} band during sliding is in contrast with the disappearance of this band due to degradation after ion radiation, as observed by Constantini et al.[34] The orientation of the *C-N*-C functional group as represented by the 1395 cm^{-1} band has a minimum value at 180°C relative to the aromatic ring structure. The progressive orientation of C═O under shear may induce additional stresses into the polymer chain, leading to a reorientation of the neighboring C-*N*-C bonds, tilting away from the sliding surface. At higher temperatures, the latter functional group again becomes more

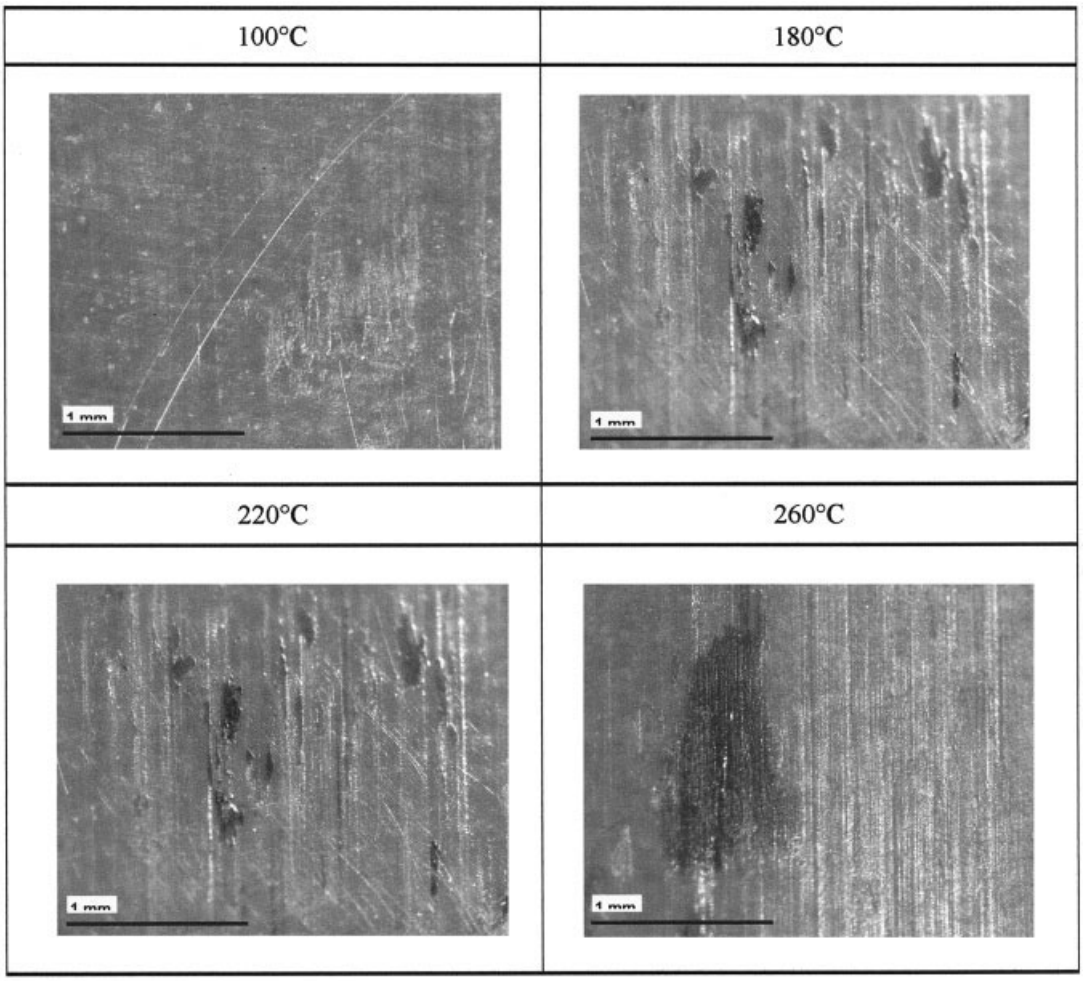

Figure 9 Optical microscopy of the worn polyimide sliding surfaces.

stretched because of enhanced molecular mobility. The opposite trends between C═O and C-*N*-C imide bonds are further confirmed by the 1395/1786 relative intensity, which also has a minimum value at 180°C. The imide III vibration (C-*N*-C transverse stretch, 1124 cm^{-1}) is weaker than the imide II vibration (C-*N*-C

TABLE IV
Band Assignments of the Peaks of FT-Raman Spectra for PAA and PI

Raman absorption band (cm^{-})	PAA poly(amic acid)	PI (polyimide)
753		Aromatic ring in dianhydride part
881	O—C═O or O═C—N (amide I)	
1124		C—N—C transverse vibration (imide III)
1247	NH bend + CH stretch (amide III)	
1330	Symmetric stretch of carboxylic acid	
1394		C—N—C axial vibration (imide II)
1565	NH bend + CH stretch (amide II)	
1601	Ring vibration of carboxylic acid	
1614		Aromatic ring in dianhydride part
1662	Carbonyl stretch (amide I)	
1685	Asymmetric carboxylate stretch	
1724	C═O stretch of free carboxylic acid	
1728		C—CO—C asymmetric stretch (imide I)
1788		C—CO—C symmetric stretch (imide I)
3070	Aromatic C—H bend	

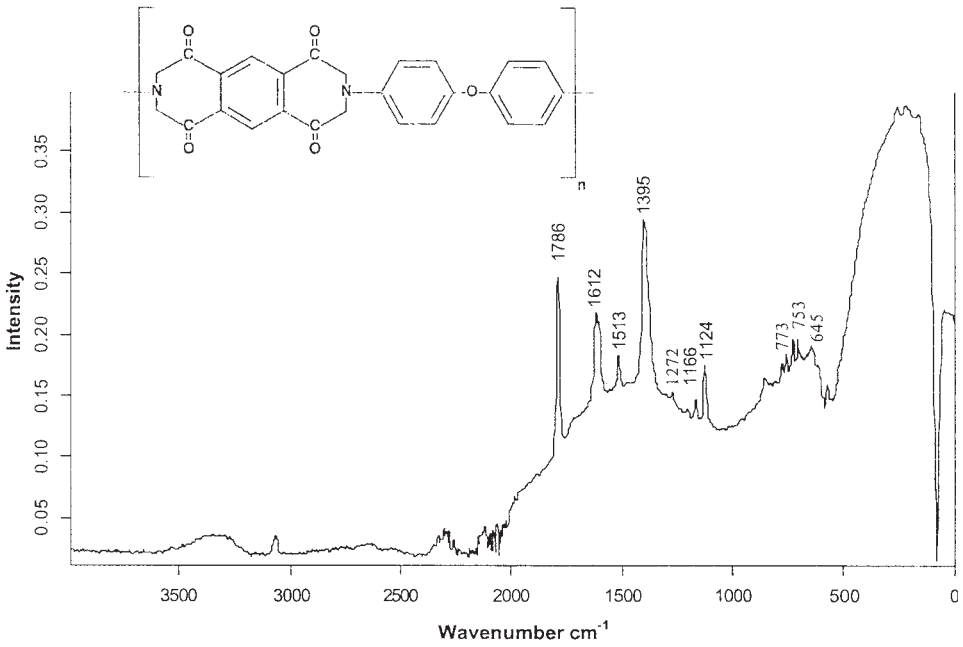

Figure 10 Characteristic Raman spectrum of unworn polyimide SP-1.

axial stretch, 1395 cm^{-1}); while the overall orientation of the axial C-*N*-C vibration progressively grows at higher bulk temperatures, its transverse orientation changes discontinuously at 180°C, explaining the previously observed maximum in friction and wear for sliding under 50*N* at 180°C. The trend of the normalized 1513 cm^{-1} band at 180°C is opposite to the 1395 cm^{-1} band; they suggest that the C═C bonding in the aromatic phenylene ring becomes tilted parallel to the sliding surface, represented by the maximum value in the 1513 cm^{-1} band. Both 1395 cm^{-1} and 1513 cm^{-1} bands seem complementary for the reorientation effects at 180°C.

The lower polyimide frequencies are rarely studied, while most important evolutions are situated at the 852 cm^{-1} (diamine ring breathing) and 773 cm^{-1} bands. The 753 cm^{-1} band is chosen as a reference band as it represents the aromatic ring in the imide part, corresponding to assignments of the 1612 cm^{-1} frequency. However, absorption bands assigned to different functions, such as C═O, ring breathing, and C-O-C stretch, overlap in this region. The 645 cm^{-1} band can be assigned to C-O-C bending, presently occurring as a bridge in the diphenylether; its intensity decreases with higher temperature, pointing towards tilting of the ether structure antiparallel to the sliding surface. The decreased intensity of the 645 cm^{-1} band at higher bulk temperature is in accordance with the decrease in the 1272 cm^{-1} band, as both are assigned to the antisymmetric stretch of the C-O-C. These assignments are presently more likely than reports of Lippert et al.,[35] who attributed this frequency peak to degradation products; while Ge et al.[31] also attributed a 1291 cm^{-1} band to phenylene-phenylene bridge stretching.

Thermal stability and temperature transitions of sintered polyimides

From previous discussion, transitions in both friction and wear evidently appear at 180°C and are correlated to reorientation effects of characteristic C═O and C-*N*-C functional groups. However, from literature they are not easily correlated to known transition temperatures of the polyimides. This problem arises because of the high thermal stability of the polyimide structure and its semithermoset characteristics. Modulated DSC of sintered polyimide is presently applied for a detailed investigation of the temperature region below 340°C on the occurrence of secondary transition temperatures. The thermogram with measurements of the specific complex heat capacity as a function of the heating temperature is shown in Figure 12, revealing two different slopes in the curve below and above 180°C. The implied sinusoidal heating regime is able to evoke thermal transitions that are not detectable by linear heating. Those transitions include not only the glass temperature T_g as an increase in the molecular moveability of the main chain and drop on mechanical properties, but rather illustrate secondary transitions below T_g where only relatively small parts or side groups locally gain rotational or vibrational freedom. They may result in local reorientation effects of, for example, the C═O side group in the polyimide structure as observed by Raman spectroscopy, while the entire polymer stiffness that is rather determined by

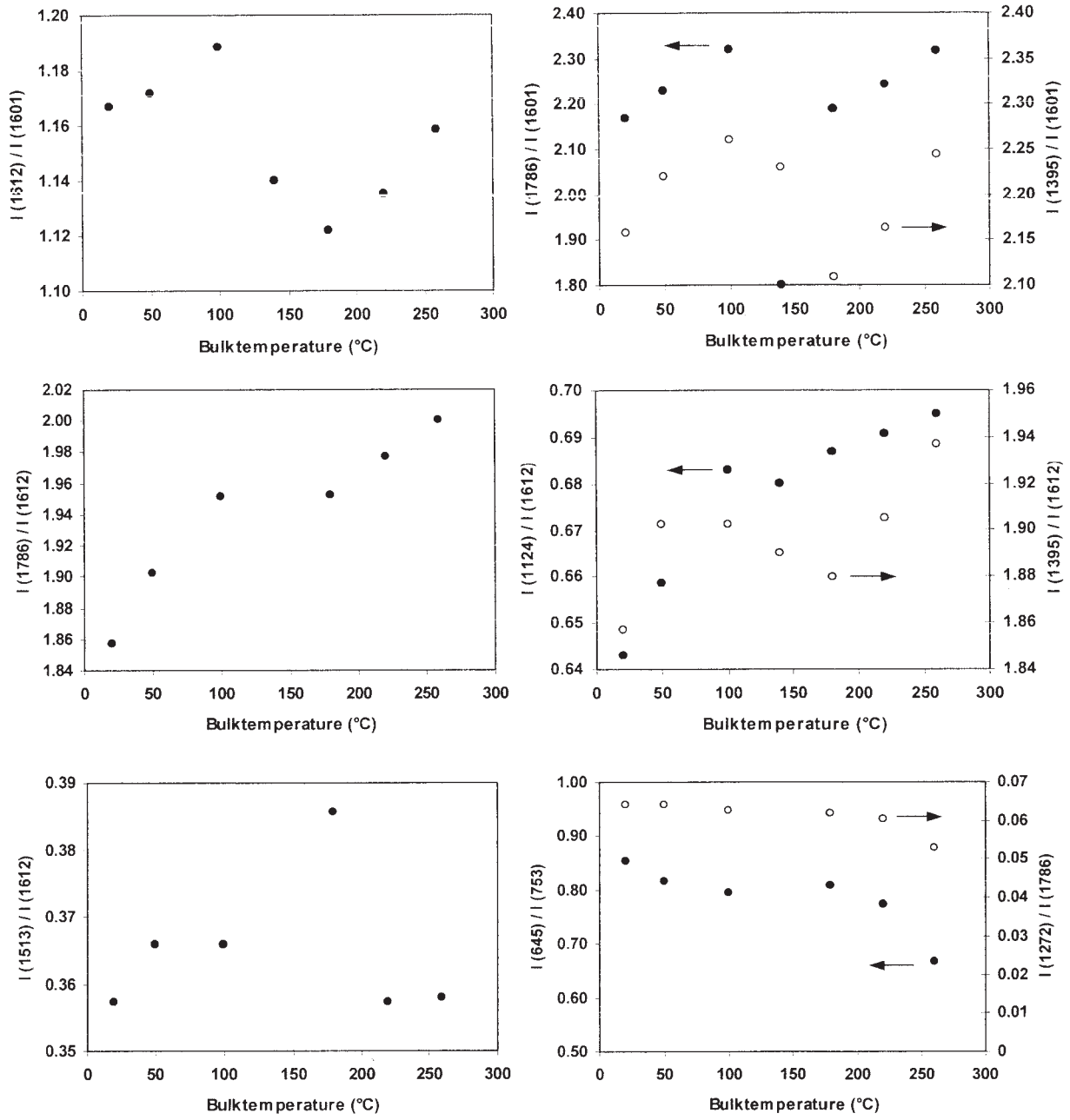

Figure 11 Relative intensities of some characteristic Raman bands as a function of bulk temperature, measured on worn polyimide surfaces after sliding under 50*N*.

the aromatic structures in the backbone of the molecular chain remains constraint.

The bulk and flash temperatures during sliding were previously calculated in Table III. The relative importance between both temperature components on the tribological properties generally depends on the test conditions[17]; at low sliding velocities and high loads the bulk temperature dominates, while high sliding velocities and lower loads enhance the importance of the flash temperature. As the observed transitions in both friction and wear occur when a bulk temperature of 180°C is applied, they correspond to a secondary transition temperature in the polyimide bulk material, while the local flash temperature remains below the decomposition temperature. This means that the bulk temperature is generally the most important factor in evoking transitions in friction and wear as it governs over longer periods of contact. Kim and Rosenblatt[36] previously discussed the effects of rubbing and temperature on the formation of an alignment layer at the surface for film materials and related the rub-induced orientation to a combination of local flash temperatures and mechanical effects. However, for present long-time sliding tests on sintered bulk

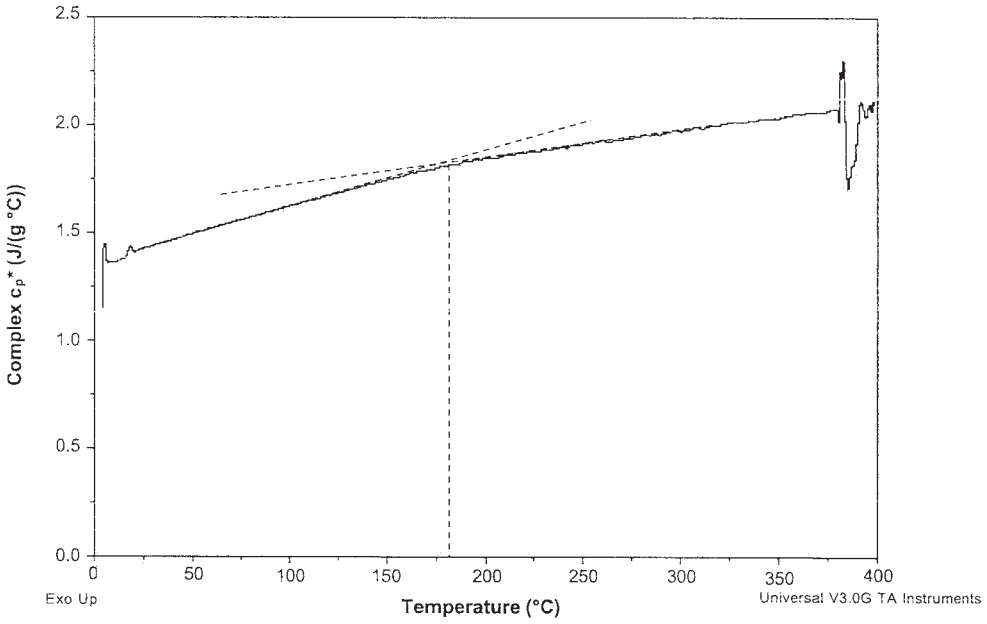

Figure 12 Complex c_p* measured by means of M-DSC on an unworn polyimide SP-1 sample.

polyimide, it is confirmed that the influence of local flash temperatures is inferior to the bulk temperature for causing tribological transitions.

CONCLUSIONS

The influence of a controlled sliding temperature between 60°C and 260°C on friction and wear of sintered polyimides (Vespel SP-1) was investigated for a fixed normal load and sliding velocity. Transitions in friction were found with a peak value at 180°C and decreasing trend at higher temperatures, which is in accordance with transitions in wear rate having a maximum value at 180°C and stabilizing at higher temperatures. At temperatures below 180°C no transfer film was detected, while the transfer film formation enlarged at higher temperatures. However, in none of the cases did a homogeneous film develop, due to the brittle nature of polyimides.

The transition temperature of 180°C observed in transfer, friction, and wear corresponds to a characteristic secondary transition temperature of sintered polyimide as measured by modulated DSC, revealing that the overall bulk temperature (artificially applied to the sliding counterface) is more important than the local flash temperature for causing variations in the tribological performance of polyimide.

By Raman spectroscopy it was demonstrated that the transitions at 180°C can be related to orientation effects of specific functional groups in the imide structure. The intensity of C-*N*-C related absorption bands is minimal at 180°C and is complementary to the intensity of the C═C phenylene structure that is maximal at 180°C. These suggest that molecules become, respectively, tilted away and parallel to the sliding surface, while the C-O-C structure slightly decreases in orientation. As thermal degradation and graphitization is unlikely at present sliding temperatures, the orientation effects of characteristic chemical bonds as observed allow for transfer film formation at temperatures above 180°C. The low wear rates measured at 140°C are possibly related to the amount of C═O functional groups in the polyimide part. Although the amount of C═O structures are minimal at 140°C, its orientation progressively enhances under sliding at elevated bulk temperatures

The authors are deeply grateful to Mr. Koen Peeters and Mr. Phillippe Cantillon from DuPont de Nemours (Mechelen, Belgium), who kindly supplied us with testing materials. Industrial Engineers, Wim Van Daele assisted us in taking the SEM photographs, and ing. Michel De Waele from the Belgian Welding Institute allowed us to perform optical microscopy.

References

1. Bahadur, S. Wear 2000, 245, 92.
2. Hollander, A. E.; Lancaster, J. K. Wear 1973, 25, 155.
3. Fusaro, R. L. Trib Trans 1988, 31, 174.
4. Tewari, U. S.; Bijwe, J. Tribological Behaviour of Polyimides, Polyimides: Fundamentals and Applications, Marcel Dekker: New York, 1996; p 533.
5. Sharf, T. W.; Singer, I. L. Trib Let 2003, 14, 3.
6. Hamrock, B. J.; Jacobson, B. O.; Schmid, S. R. Fundamentals of Machine Elements; WCB/McGraw-Hill: Boston, 1999.
7. Friedrich, K. Trib Int 1989, 22, 25.
8. Schawe, J. E. K. Thermochim Acta 1995, 260, 1.

9. Kanari, K.; Ozawa, T. Thermochim Acta 2003, 399, 189.
10. Bhushan, B. Principles and Applications of Tribology; Wiley-Interscience: New York, 1999.
11. Tanaka, K.; Ueda, S. J Jpn Soc Lubr Eng 1980, 26, 62.
12. Chitsaz-Zadeh, M. R.; Eiss, N. S. Wear 1986, 110, 359.
13. Blok, H. Wear 1963, 6, 483.
14. Archard, J. F. Wear 1958, 2, 438.
15. Tian, X.; Kennedy, F. E. ASME. J Trib 1994, 116, 167.
16. Greenwood, J. A.; Alliston-Greiner, A. E. Wear 1992, 155, 269.
17. Ashby, M. F.; Abulawi, J.; Kong, H. Background Reading: Frictional Heating at Dry Sliding Surfaces; Cambridge Press: Cambridge, 1992.
18. Jaeger, C. J. Proc R Soc NSW 1942, 76, 1107.
19. Dupont Co., Vespel Parts and Shapes, Design Handbook, Dupont Engineering Polymers: Geneva, 2000.
20. Iwabuchi, A.; Hori, K.; Sugawara, Y. Wear 1988, 125, 67.
21. Cong, P. H.; Li, T. S.; Liu, X. J.; Zhang, X. S.; Xue, Q. J. Acta Pol Sinica 1988, 5, 556.
22. Cincovic, M. M.; Babic, D.; Jovanovic, R.; Popov-Pergal, K.; Pergal, M. Polym Degrad Stab 2003, 81, 387.
23. Pozdnyakov, A. O.; Kudryavtsev, V. V.; Friedrich, K. Wear 2003, 254, 501.
24. Matsubara, K.; Wanatabe, M.; Karasawa, M. Junkatsu 1969, 14, 43.
25. Tanaka, K.; Yamada, Y. Proc ACS Symp Series; Lee, L. H., Ed. 1985, 287, 103.
26. Fusaro, R. L. ASLE Trans 1978, 21, 125.
27. Bill, R. C. Wear 1985, 106, 283.
28. Paek, S. H.; Durning, C. J.; Lee, K. W.; Lien, A. J Appl Phys 1998, 83, 1270.
29. Walsh, T. R.; Harkins, C. G.; Sutton, A. P. J Chem Phys 2000, 112, 4402.
30. Raimondi, F.; Abolhassani, S.; Brutsch, R.; Geiger, F.; Lippert, T.; Wambach, J.; Wei, J.; Wokaun, A. J Appl Phys 2000, 88, 3659.
31. Ge, J.; Xue, G.; Li, F.; McCreight, K.; Wang, S.; Harris, F.; Cheng, S.; Zhuang, X.; Hong, S.; Shen, T. Macromol Rapid Commun 1998, 19, 619.
32. Yu, K. H.; Yoo, Y. H.; Rhee, J. M.; Lee, M. H.; Yu, S. C. Bull Korean Chem Soc 2003, 24, 357.
33. Fukuhara, M. J Appl Polym Sci 2003, 90, 759.
34. Constantini, J. M.; Couvreur, F.; Salvetat, J. P.; Bouffard, S. Nucl Instrum Methods Phys Res Sect B 2002, 194, 132.
35. Lippert, T.; Ortelli, E.; Panitz, J. C.; Raimondi, F.; Wambach, J.; Wokaun, A. Appl Phys A 1999, 69, S651.
36. Kim, J. H.; Rosenblatt, C. J Appl Phys 2000, 87, 155.